

# Microstructure and Mechanical Properties of Weld Fusion Zones in Modified 9Cr-1Mo Steel

M. Sireesha, Shaju K. Albert, and S. Sundaresan

(Submitted 25 September 2000)

Modified 9Cr-1Mo steel finds increasing application in power plant construction because of its excellent high-temperature properties. While it has been shown to be weldable and resistant to all types of cracking in the weld metal and heat-affected zone (HAZ), the achievement of optimum weld metal properties has often caused concern. The design of appropriate welding consumables is important in this regard. In the present work, plates of modified 9Cr-1Mo steel were welded with three different filler materials: standard 9Cr-1Mo steel, modified 9Cr-1Mo, and nickel-base alloy Inconel 182. Post-weld heat treatment (PWHT) was carried out at 730 and 760 °C for periods of 2 and 6 h. The joints were characterized in detail by metallography. Hardness, tensile properties, and Charpy toughness were evaluated. Among the three filler materials used, although Inconel 182 resulted in high weld metal toughness, the strength properties were too low. Between modified and standard 9Cr-1Mo, the former led to superior hardness and strength in all conditions. However, with modified 9Cr-1Mo, fusion zone toughness was low and an acceptable value could be obtained only after PWHT for 6 h at 760 °C. The relatively poor toughness was correlated to the occurrence of local regions of untransformed ferrite in the microstructure.

**Keywords** mechanical properties, microstructures, modified 9Cr-1Mo steel, welding

## 1. Introduction

Efforts to raise the thermal efficiency of advanced power generation systems have resulted in a trend toward the use of higher operating temperatures and pressures.<sup>[1–3]</sup> This calls for the development of new constructional materials with improved high-temperature properties. The family of 9Cr-1Mo steels is one of the most promising among the candidate materials for such applications.<sup>[4]</sup> Starting with the standard 9Cr-1Mo steel, considerable improvement in mechanical properties has been achieved by the addition of small amounts of vanadium and niobium. Many reports have indicated that the Nb/V containing “modified 9Cr-1Mo” steel (often designated as T91 for tubing and P91 for piping) offers tensile and creep properties superior to those of other ferritic steels.<sup>[5–7]</sup> The P91 steel owes its excellent mechanical properties to a distribution of fine-sized incoherent niobium and vanadium carbonitride precipitate particles and an optimized Nb/V ratio.<sup>[8]</sup>

The creep strength of the modified 9Cr-1Mo steel is higher than that of most of the Cr-Mo steels ranging from 2.25Cr-1Mo to 12Cr-1Mo over the entire creep temperature range.<sup>[5]</sup> In terms of yield strength and ultimate tensile strengths (UTS) as well as creep rupture strength, the modified 9Cr-1Mo steel is superior to the standard 9Cr-1Mo steel and other ferritic materials from room temperature up to approximately 700 °C.<sup>[9]</sup> Some advantages for P91 over type 304 austenitic stainless

steel up to 625 °C have also been suggested.<sup>[10]</sup> In addition to high creep strength, P91 also exhibits good ductility and toughness, adequate resistance to cracking during welding, and a low coefficient of thermal expansion.<sup>[5]</sup> The modified 9Cr-1Mo steel thus finds increasing use in steam generators, fast breeder reactors, and other applications involving temperatures higher than 500 °C.<sup>[11]</sup>

Welding is an important means of fabrication for many of these applications, and, hence, the welding characteristics of P91 constitute an important criterion for its selection. It has been shown that P91 can be welded satisfactorily by many processes including manual metal arc, submerged arc, and gas tungsten-arc welding.<sup>[12]</sup> Postweld heat treatment (PWHT) is necessary for tempering the martensite formed during welding, and many investigations have highlighted the need for optimizing the PWHT temperature and time as well as filler material composition.<sup>[12,13]</sup> The development of welding consumables that would result in optimum weld metal properties (after PWHT) with respect to both creep strength and toughness is an important consideration.

The behavior of the heat-affected zone (HAZ) has been studied using thermal simulation techniques, and it has been found that the impact toughness is generally lowered as a result of the weld thermal cycle, especially for longer cooling periods through the transformation range.<sup>[14]</sup> It would therefore be beneficial to limit the heat input for ensuring a sufficiently short cooling time. A reduction in creep strength of simulated HAZs has also been reported, which has been attributed to changes in precipitate morphology, particularly of the vanadium nitride particles.<sup>[15]</sup> However, no susceptibility to reheat cracking has been noticed in the coarse-grained HAZ, and it has been shown further that the P91 material does not show any tendency to solidification or liquidation cracking.<sup>[14]</sup>

While the modified 9Cr-1Mo steel is thus known to be weldable and is not susceptible to weld or HAZ cracking of any kind, the achievement of adequate properties in the weldment

M. Sireesha and S. Sundaresan, Department of Metallurgical Engineering, Indian Institute of Technology, Madras-600 036, India; and Shaju K. Albert, Materials Technology Division, Indira Gandhi Centre for Atomic Research, Kalpakkam-603102, India. Contact e-mail: sundaresaniyer@hotmail.com.

**Table 1 Chemical composition of materials used, wt.%**

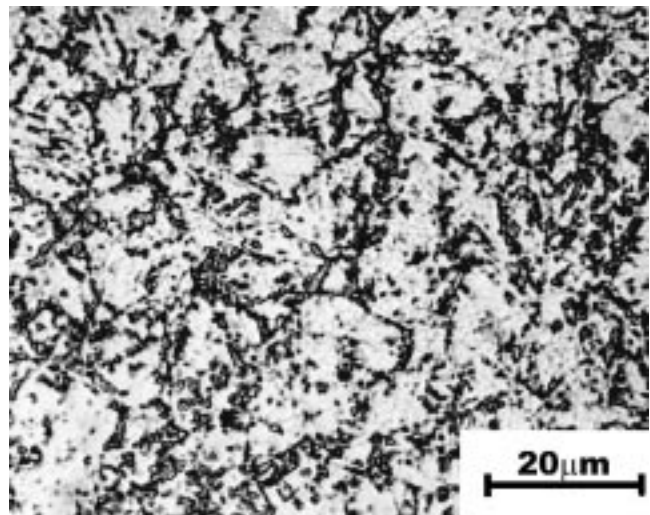
Element	← Undiluted weld deposit →				
	P91 base metal	P9 filler	P91 filler	Inconel 182 filler	Weld metal with P91 filler
C	0.05	0.05	0.11	0.04	0.11
Cr	9.14	8.69	9.1	14.28	8.94
Ni	0.42	0.05	0.65	69.51	0.75
Mo	0.96	0.96	1.0	...	0.89
Mn	0.37	0.61	0.7	7.38	0.57
Si	0.26	0.13	0.35	0.49	0.22
P	0.01	0.02	<0.007	0.01	0.011
S	0.001	0.01	0.008	0.001	0.007
N	...	...	0.03	...	0.03
V	0.25	0.02	0.14	...	0.17
Al	0.01	0.002	0.022	...	0.02
Nb	0.09	0.01	0.09	1.64	0.04
Ti	0.002	0.01	0.01	0.34	0.03
Fe	Bal	Bal	Bal	Bal	Bal

continues to present some concern. Further, little work has been reported with regard to microstructural changes during welding and during subsequent heat treatment and their influence on the properties obtained. In the current work, welded joints were produced in P91 using three different types of filler materials, and PWHT was carried out under different conditions. Detailed metallographic characterization enabled a correlation among weld metal composition, microstructure, and mechanical properties. Important conclusions could thus be drawn regarding the choice of filler material and PWHT conditions.

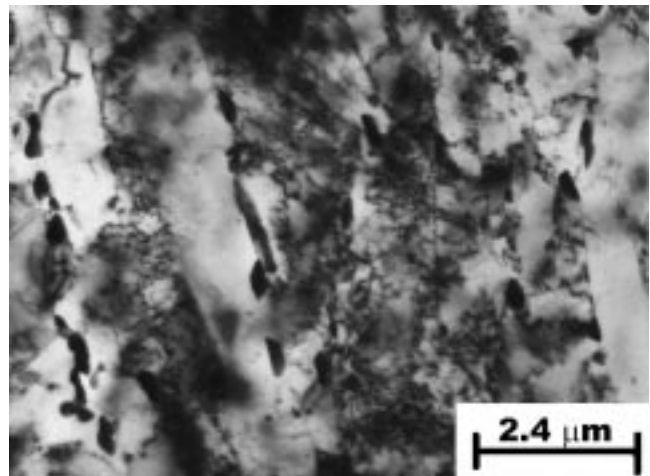
## 2. Experimental Details

The base material used in the present investigation was a 12 mm thick plate of modified 9Cr-1Mo steel, whose composition is given in Table 1. It was supplied in the normalized (1080 °C) and tempered (750 °C/1 h) condition. The welding process employed was manual metal arc welding. The base plates were butt-welded with an included angle of 60° using three types of consumables, *viz.*, the standard 9Cr-1Mo steel (P9), modified 9Cr-1Mo steel (P91), and Inconel 182 (Inconel is a trademark of INCO Alloys International, Huntington, WV), whose chemical compositions determined from undiluted weld deposits are also shown in Table 1. The P9 filler material is sometimes considered for welding of P91 to itself, particularly for the root pass.<sup>[16]</sup> Inconel 182 was also employed in the present study because it is the recommended filler material for dissimilar welds involving P91 as one of the base materials and it would therefore be useful to study microstructural features associated with its use. The preheat and interpass temperature employed was 250 °C. The weldments were subjected to PWHT at two different temperatures, *viz.*, 730 and 760 °C, for durations of 2 and 6 h at each temperature. These conditions were selected to be in accordance with recommended welding practice. Most fabricators specify 760 °C for 2 h, but individual specifications require lower temperatures for longer times.<sup>[13]</sup>

Room-temperature toughness evaluation was carried out using standard Charpy specimens with the welding direction as the direction of crack propagation. All weld longitudinal tensile specimens were tested in an Instron 1195 unit at room



(a)



(b)

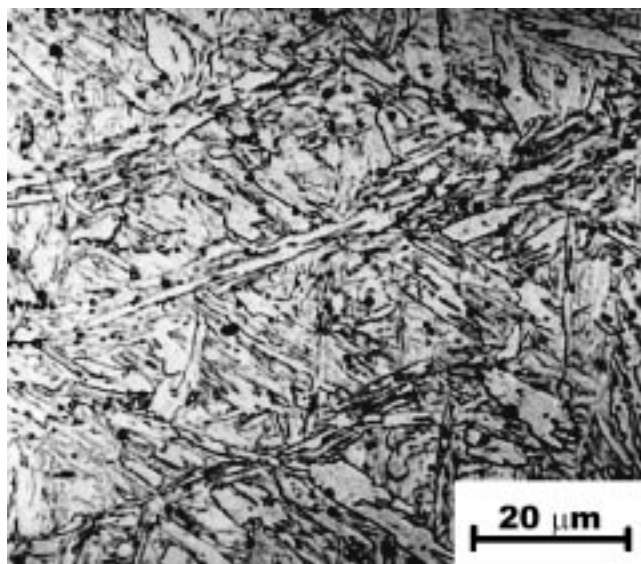
**Fig. 1** (a) Micrograph of as-received (normalized and tempered) base material. (b) Transmission electron microscopy (TEM) micrograph of as-received base material

temperature at a nominal strain rate of  $3 \times 10^{-4}$ /s. Hardness measurements across the weldments were made using the Vickers hardness tester at a constant load of 3 kg. For metallographic examination, the etching solutions used were Vilella's reagent for iron-base weld metals and oxalic acid (electrolytic etching) for nickel-base weld metals. For revealing carbides, electrolytic etching in a 23% ammonia solution at 4 V for 5 s was found suitable. For transmission electron microscopy, slices of 1 mm thickness, lying entirely in the fusion zone, were thinned to about 50 m using emery papers. Electrolytic thinning was carried out in two stages, *viz.*, with the window technique and with twin-jet electropolishing. In both the techniques, the electrolyte was a mixture of 80% methanol and 20% perchloric acid.

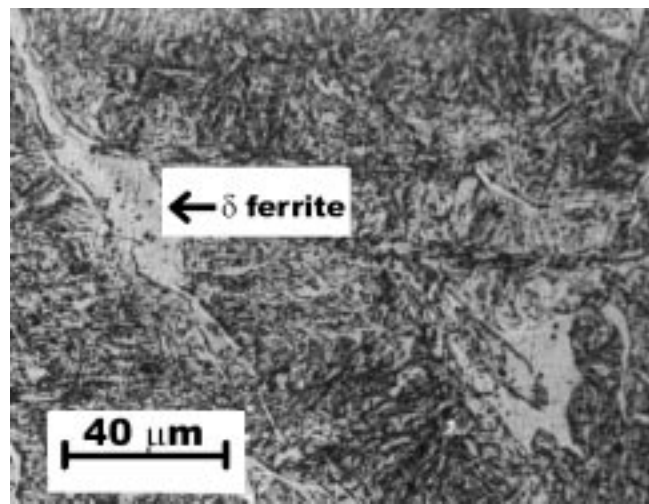
## 3. Results and Discussion

### 3.1 Microstructures

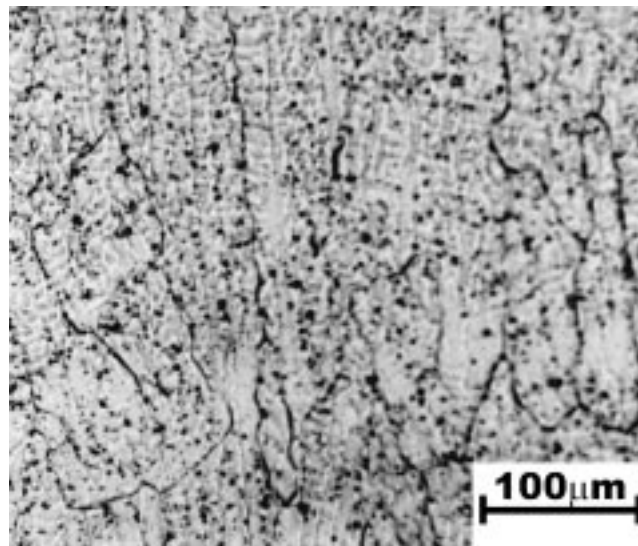
In the as-received normalized and tempered condition, the microstructure of the P91 base metal (Fig. 1a) consists of fully



(a)



(b)



(c)

**Fig. 2** (a) Micrograph of P9 weld metal in as-welded condition. (b) Micrograph of P91 weld metal in as-welded condition. (c) Micrograph of Inconel 182 weld metal in as-welded condition

tempered martensite with small precipitate particles on the prior austenite grain boundaries and some within the grains, which could be observed even in the light microscope at 1000 $\times$  magnification. The transmission electron micrograph of the base metal (Fig. 1b) shows a lath martensitic structure, with a number of precipitate particles lying along the lath boundaries, which are presumably of the  $M_{23}C_6$  type identified in earlier studies.<sup>[5,17,18]</sup> Additionally, much finer precipitate particles of niobium-rich or vanadium-rich compounds could also be observed both along the boundaries and within the laths. Although the material has been tempered at 750 °C for 1 h, the high dislocation density characterizing the as-normalized material is still not appreciably decreased.

The microstructures of the three weld metals produced with

P9, P91, and Inconel 182 electrodes are shown in Fig. 2(a) to (c). In the as-welded condition, both the P9 and P91 electrodes produce a predominantly martensitic structure in which the solidification substructures characteristic of weld fusion zones are not seen. These weld metals solidify as ferrite in which the rapid diffusion allows considerable compositional homogenization. Furthermore, subsequently, other transformations (from ferrite to austenite and austenite to martensite) also occur in the solid state. These have prevented the observation of the solidification substructure in these welds. The nickel-based Inconel 182 weld metal, on the other hand, reveals more clearly the cellular dendritic structure commonly found in weld metals. A particularly important feature of interest in the P91 weld metal is the occurrence of patches of ferrite, as indicated in

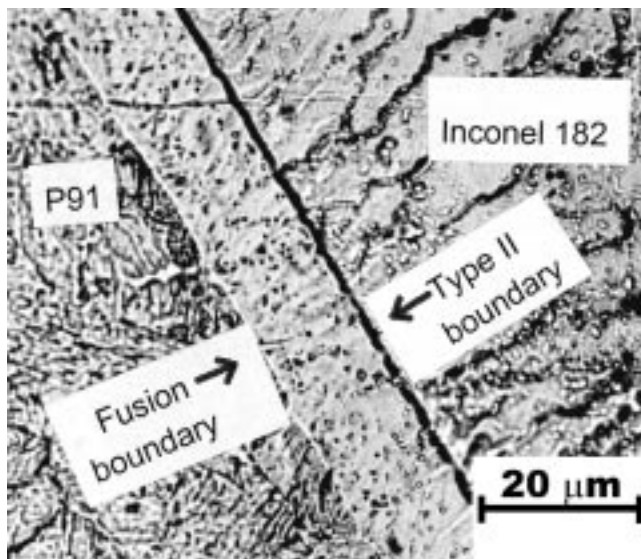


**Fig. 3** Microstructure showing type II boundary at Inconel 182/P91 interface

Fig. 2(b). This has undesirable consequences as regards the toughness of the weld metal and is discussed later in the text.

The interface between the nickel-base weld metal and the ferritic steel base metal (Fig. 3) shows the presence of a long, nearly straight grain boundary parallel to the fusion boundary and within the weld metal. Such a feature is characteristic of dissimilar metal welds and has been identified as type II boundaries.<sup>[19]</sup> These are different from type I boundaries usually observed in homogeneous (similar base and filler materials) welds, in which epitaxial growth causes grain boundaries from the base metal substrate to run continuously across the fusion boundary in a direction roughly perpendicular to it. The occurrence of type II boundaries was originally attributed to a transition in solidification behavior (say from ferritic to austenitic) due to the compositional gradient normal to the fusion boundary. More recent work<sup>[19]</sup> has shown that the type II boundary is a result of allotropic transformation (say from  $\delta$  to  $\gamma$ ) in the base metal that occurs on cooling and produces mobile grain boundaries of the  $\gamma/\gamma$  type at the fusion boundary in dissimilar metal (fcc/bcc) welds. It has been shown that type II boundaries can form in such dissimilar metal welds only when there is a ferrite/austenite phase boundary at elevated temperature in the base metal. In the present work, the Inconel 182 weld metal solidifies in the austenitic mode in spite of the dilution from the base metal, while the P91 parent material solidifies as ferrite and then undergoes transformations first to austenite and then to martensite.

Transmission electron microscopy was also performed on the P9 and P91 weld metal specimens, and Fig. 4(a) and (c) show the micrographs in the as-welded condition. Both microstructures exhibit lath martensite with a high dislocation density. The micrographs also show the presence of fine needle-shaped precipitates, a greater density of precipitation being visible in the P91 material than in P9. This indicates that a limited extent of autotempering has occurred during cooling of the weld metals. Such autotempering is possible in view of the relatively

high martensite transformation temperature ( $M_s \sim 400$  °C) in these steels.<sup>[20]</sup>

The microstructures of the P9 and P91 weldments after tempering at 760 °C for 6 h are shown in Fig. 5(a) and (b). Evidence of precipitation can be noticed in these light optical micrographs. The distribution of carbide precipitate particles in the tempered material can be observed more clearly by etching electrolytically with 23% ammonia solution. Figure 6 is one such micrograph for the P91 weld metal after tempering at 730 °C for 2 h. Fine carbide particles are seen to be distributed not only along the previous austenite grain boundaries but also throughout the matrix.

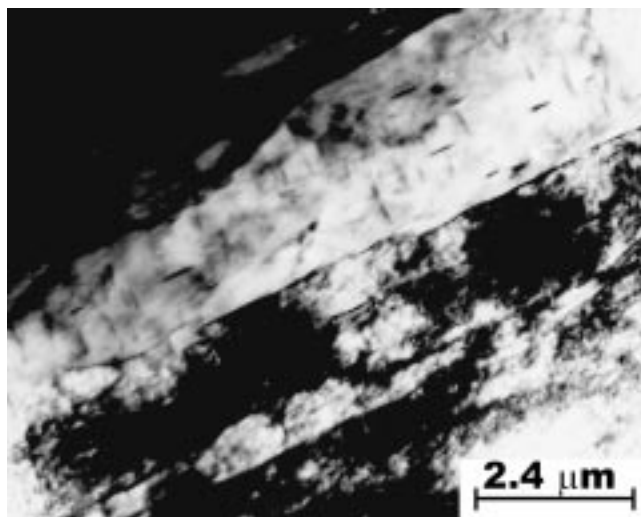
The transmission electron micrographs of the postweld heat-treated P9 and P91 weld metal specimens are reproduced in Figs 7(a) to (d). These reveal the lath structure of the tempered martensite as in the case of the base material (Fig. 1b). Precipitation of carbides and other particles is seen to have occurred along prior austenite grain boundaries, along lath interfaces, and also within the laths. A somewhat greater degree of lath boundary precipitation characterizes the tempered structure in P91. Similarly, with P91 weld metal, the precipitation along lath interfaces appears to be more continuous after the 760 °C/6 h treatment than after 2 h at 730 °C. There is a greater tendency toward a reduction in dislocation density after the tempering treatment at 760 °C/6 h than after the treatment at 730 °C/2 h. A comparison of P9 and P91 weld metals after the higher temperature tempering (Fig. 7(b) and (d)) shows evidence of polygonization in P9 but not in P91. However, in the case of P91, a closer observation of Fig. 7(d) reveals the beginning of lath breakup.

In the HAZ, depending on the peak temperature reached in the various regions, the material is taken to one of several subsolidus phase fields in the Fe-Cr-Mo-C system:  $\alpha$  + carbides,  $\alpha$  +  $\gamma$  + carbides,  $\gamma$ , and  $\alpha$  +  $\gamma$ . In the as-welded condition, the structure would be predominantly martensitic, which would undergo tempering during PWHT. Figures 8(a) and 8(b) show the coarse-grained and fine-grained HAZ regions after tempering at 730 °C at 2 h. These reveal tempered martensite, but the grain size even in the coarse-grained HAZ is much smaller than in the fusion zone. The HAZ microstructures show additionally a few isolated grains of ferrite, some of the ferrite formed during heating to peak temperature remaining untransformed during cooling.

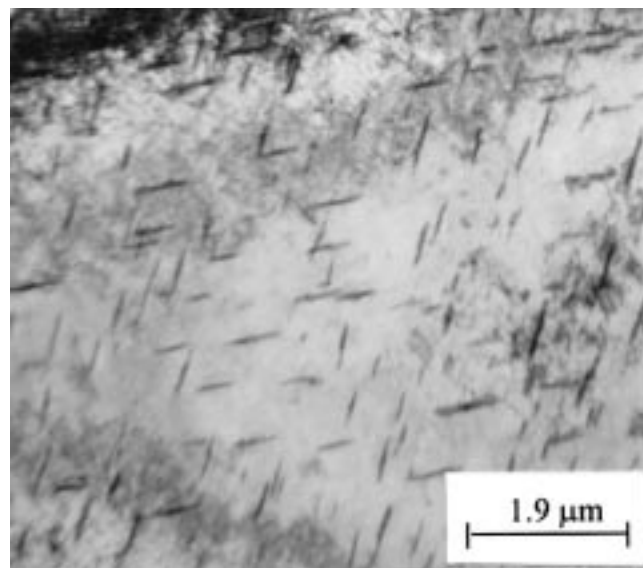
In the case of the Inconel 182 weld metal, there was no change observed in the microstructure due to PWHT. The microstructural stability of nickel-base alloys at elevated temperatures is well known. In an earlier investigation on the behavior of nickel-based weld metal during PWHT in the 600 to 900 °C temperature range,<sup>[21]</sup> embrittling precipitation was found to occur at 700 °C, but only after aging for 10,000 h. Precipitation was less pronounced at 600 °C and even less in the range 800 to 900 °C. It is therefore not surprising that the nickel-base weld metals did not exhibit any microstructural change during PWHT for 2 and 6 h at 730 and 760 °C, respectively.

### 3.2 Hardness

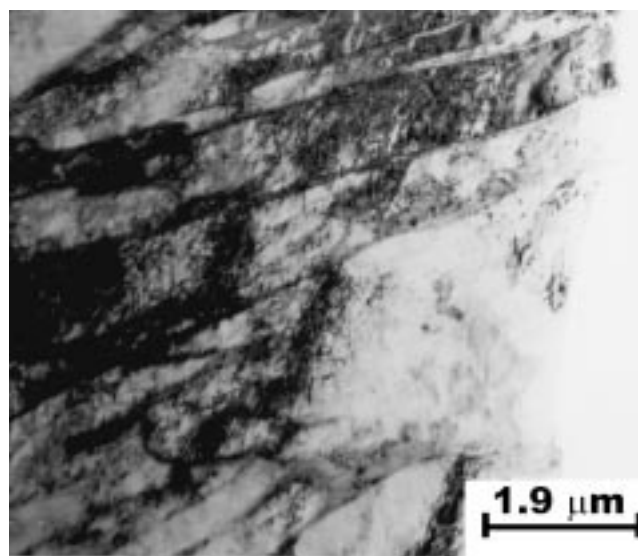
The hardness distributions across the welded joint in the as-welded and heat-treated conditions for the different filler materials used are given in Fig. 9(a) to (c). In the as-welded



(a)



(b)



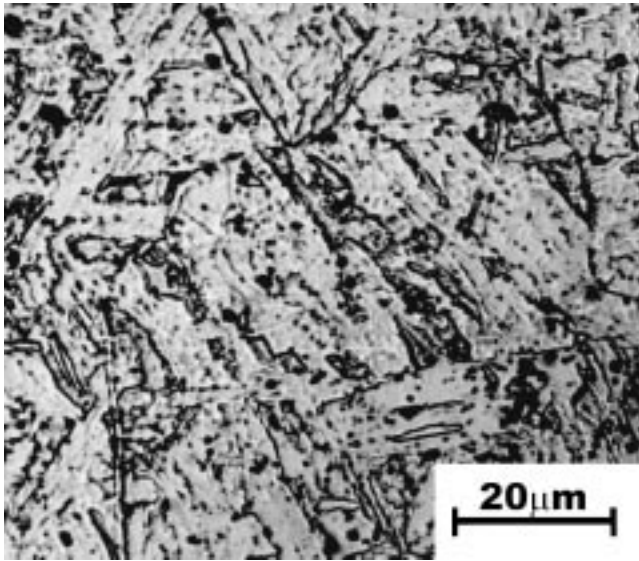
(c)

**Fig. 4** (a) TEM micrograph of P9 weld metal in as-welded condition. (b) TEM micrograph of P91 weld metal in as-welded condition. (c) TEM micrograph of P91 weld metal in as-welded condition

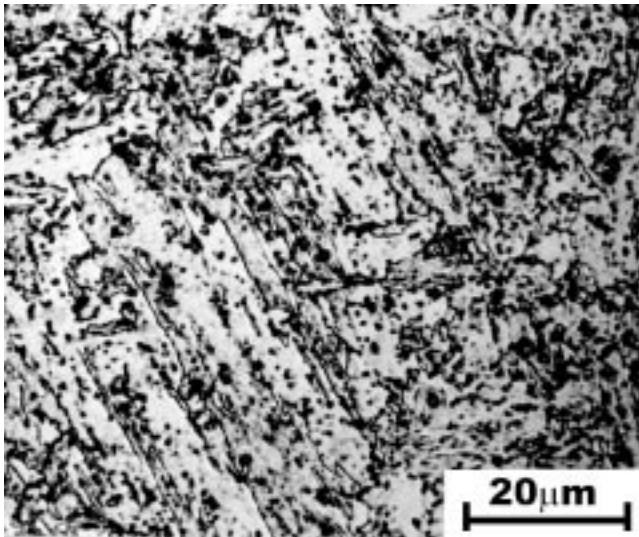
condition, both the 9Cr-1Mo welds exhibit high hardness because of their martensitic structure, when compared to the Inconel 182 weld metal, which shows a low hardness of about 170 to 180 VHN, characteristic of austenitic welds. The as-welded hardness of the P9 fusion zone is lower than that of the P91, presumably as a result of its lower interstitial content. In the HAZ, the as-welded hardness close to the fusion boundary is high, as the material in this region has been austenitized and retransformed to martensite. Farther away, the hardness quickly drops to that of the original base material, *i.e.*, about 245 VHN.

After PWHT, the hardness of both the 9Cr-1Mo weld metals is lowered as a result of the tempering reactions, which include a reduction in dislocation density, lath break-up and development of a polygonized structure, reduction in solid solution

strengthening due to precipitation, and coarsening of precipitates.<sup>[20,22]</sup> It is important to note that the tempering treatment at 730 °C/2 h has not led to an appreciable decrease in the fusion zone hardness in the case of P91, whereas a significant reduction was experienced by the P9 welds during the same treatment. In the P91 weldment, it is only after the 760 °C/6 h treatment that the fusion zone hardness is lowered to a value approaching that of the base material. The Inconel 182 weld metal, on the other hand, being fully austenitic, undergoes practically no change in the hardness because of the absence of any significant metallurgical reactions for the conditions employed in the heat treatments. Post-weld heat treatment, however, results in a drop in hardness in the HAZ similar to the other two cases.



(a)



(b)

**Fig. 5** (a) Micrograph of P9 weld metal after tempering at 760 °C/6 h. (b) Micrograph of P91 weld metal after tempering at 760 °C/6 h

### 3.3 Tensile Properties

In order to compare the effects of the different filler materials and the postweld heat-treated conditions on yield strength and UTS; longitudinal all-weld tensile specimens were extracted from the various fusion zones. The results of these tensile tests are summarized in Table 2. The base metal tensile properties are also included in the table for comparison.

The yield strength and UTS exhibited by P9 and P91 weld metals in the as-welded condition are appreciably greater than those of the base metal, but the tensile elongations are much lower. This increased strength is attributed to the presence of an untempered lath martensitic structure pinned by a large number of dislocations. The PWHT reduces strength and generally improves ductility, these effects becoming more significant

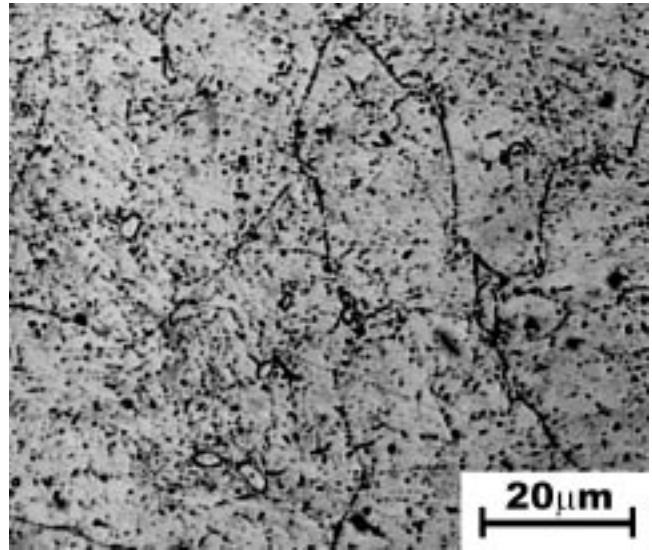


**Fig. 6** Carbides in P91 weld metal after tempering at 730 °C/2 h

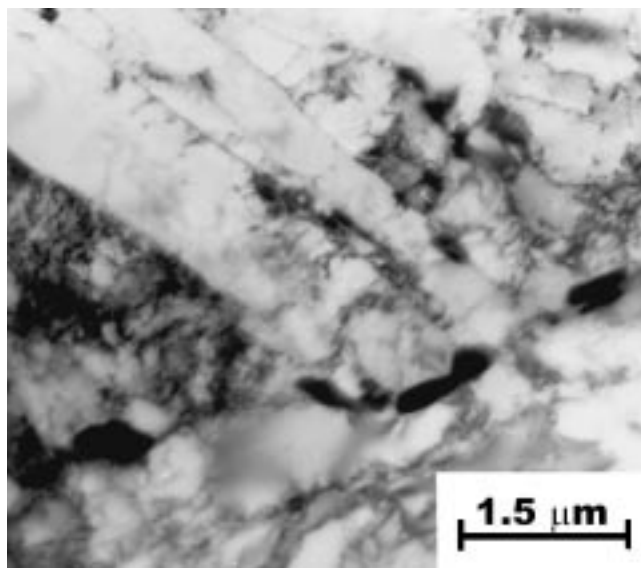
as the tempering time and temperature are increased. An important observation is that, in the P91 fusion zone, the strength reduction consequent to tempering at 730 °C for 2 h is much less pronounced than in the case of P9. Even after this tempering treatment, the P91 weld has a yield strength of 873 MPa and a UTS of 960 MPa; this is accompanied by a tensile elongation that is surprisingly even lower than in the as-welded condition, even though the percentage reduction in area increases well above the as-welded condition. It is only after a 6 h treatment at 760 °C that the strength values are similar to those of the parent material and the ductility rises to 11.2%. It is worthwhile to recall that the hardness plots also show that softening of the P91 weld during post-weld tempering becomes pronounced only at 760 °C for 6 h. A comparison of the behavior of P9 and P91 filler materials shows that, in all PWHT conditions, the P91 welds exhibit much higher strength but lower ductility.

It must be pointed out that, even after a tempering treatment at 760 °C for as long as 6 h, the tensile elongations of both P9 and P91 weld metals are still only 14% and 11.2%, respectively. These are much lower than the usual value of about 20% that has been quoted in the literature.<sup>[12,23]</sup>

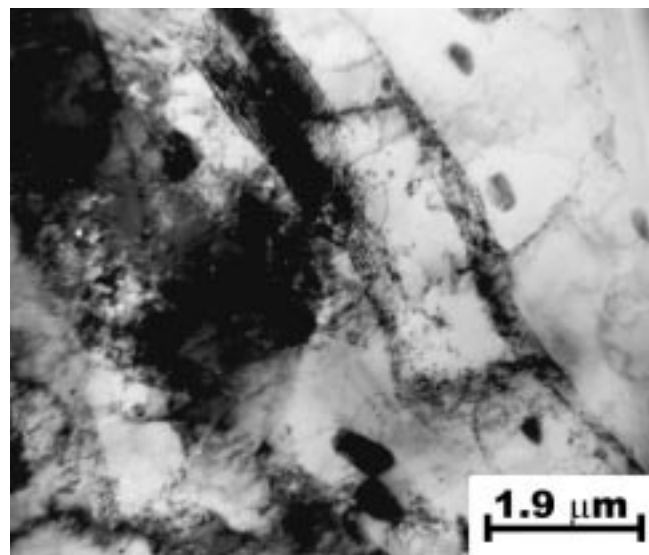
On the contrary, the picture is much different in the case of the Inconel 182 weld metal. In the as-welded condition, as opposed to the P9 and P91 weldments, the strength values are much lower but ductility is very high, the tensile elongation reaching nearly 40%. The PWHT produces marginal increases in strength and a reduction in ductility, but these effects are quite insignificant. As explained when discussing hardness plots, the Inconel 182 weld metal is known to be metallurgically stable and treatments for a few hours in the temperature range 730 to 760 °C are unlikely to cause any metallurgical reactions. Metallographically, also no change could be detected in this weld metal during the PWHTs employed.

### 3.4 Toughness

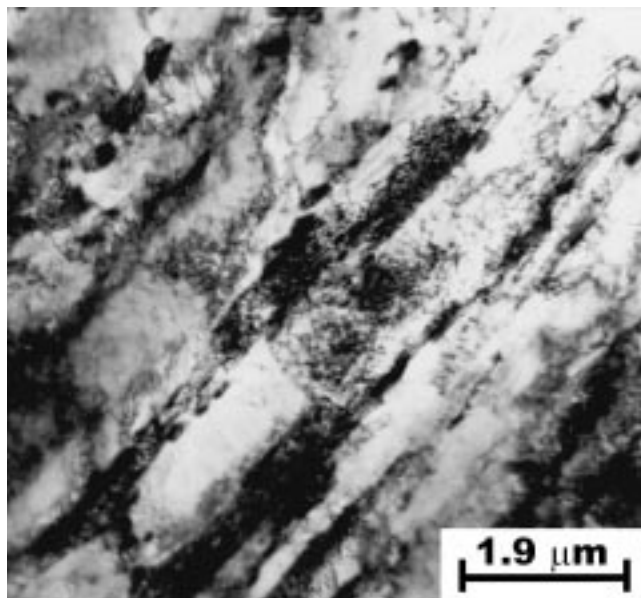
The results of room-temperature Charpy impact testing are given in the form of a bar chart in Fig. 10. The P9 and P91



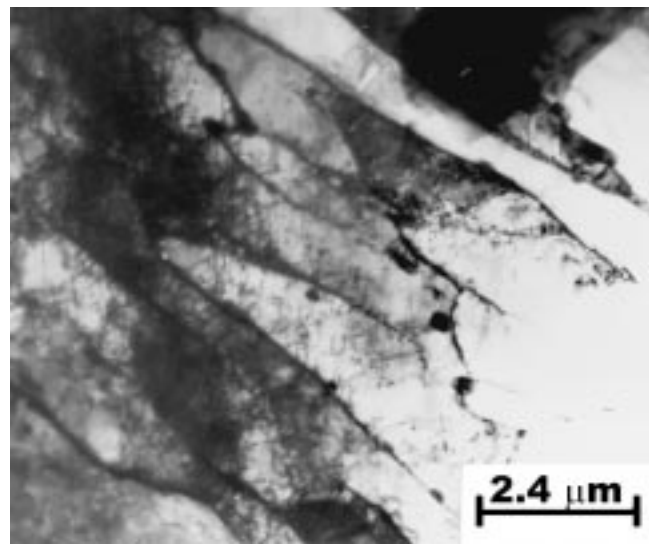
(a)



(b)



(c)



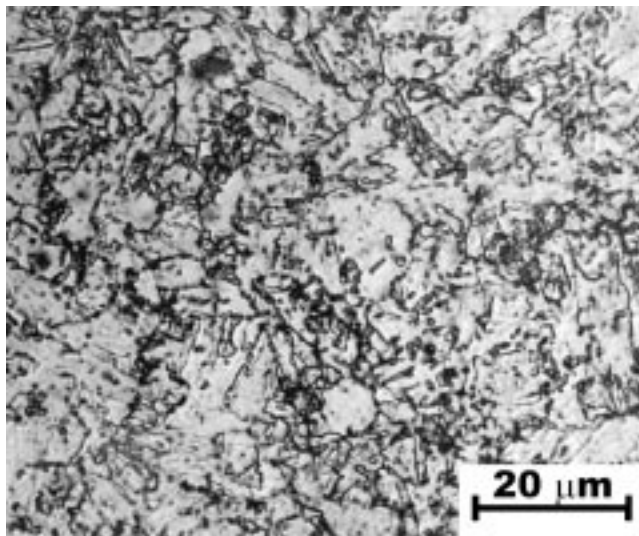
(d)

**Fig. 7** (a) TEM micrograph of P9 weld metal after tempering at 730 °C/2h. (b) TEM micrograph of P9 weld metal after tempering at 760 °C/6 h. (c) TEM micrograph of P91 weld metal after tempering at 730 °C/2 h. (d) TEM micrograph of P91 weld metal after tempering at 760 °C/6 h

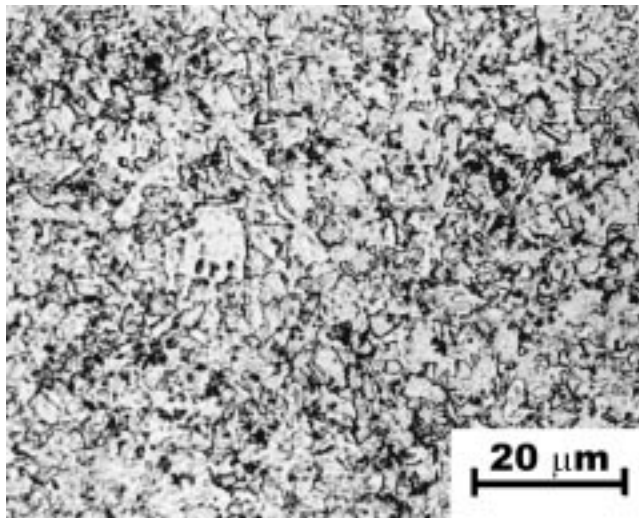
welds exhibit a poor toughness of less than 20 J in the as-welded condition. The absorbed energy increases, however, on PWHT, and this effect becomes progressively greater as tempering time and temperature are increased. The P9 and P91 welds exhibit similar behavior except that the P91 weld shows a slightly higher toughness after the 760 °C/6 h treatment. The increase in toughness on PWHT is no doubt a consequence of the tempering reactions already discussed. Here again, however, it must be pointed out that the toughness values obtained in the current investigation are lower than those reported in the literature for corresponding heat treatments.<sup>[13,23]</sup> Also, the ISO specification<sup>[12]</sup> calls for a minimum toughness of 41 J, and the IGCAR specification for the Prototype Fast Breeder Reactor<sup>[24]</sup>

stipulates a minimum of 45 J for the postweld heat-treated welds. Figure 10 shows that these minimum values have been achieved by the P9 and P91 welds in the current investigation only after a PWHT at 760 °C for 6 h. The poor toughness exhibited by these welds after the lower temperature tempering (especially the 730 °C/2 h treatment) is in accordance with their poor tensile elongation in the same heat-treated condition. In the case of the Inconel 182 weld metal, the as-welded condition itself is characterized by a much greater toughness of nearly 100 J, and this remains substantially unaltered by any of the four tempering treatments employed. This again demonstrates the metallurgical stability of the nickel-base weld metal.

Among the three filler metals used, although Inconel 182



(a)



(b)

**Fig. 8** (a) Coarse-grained HAZ in a P91 weldment. (b) Fine-grained HAZ in a P91 weldment

yields excellent ductility and toughness even in the as-welded condition, its strength values are much undermatched with respect to the base metal. Between P9 and P91, while P9 exhibits better ductility, its yield strength and UTS are lower than in the case of P91 in all conditions. Additionally, the creep properties of welds made with the P9 filler may be expected to be inferior to the welds with P91. These factors are also not compensated by superior toughness; in fact, the P9 weld shows even lower toughness than the P91 weld after tempering for 6 h at 760 °C. From these points of view, P91 would appear to be the optimal filler material. However, it must be emphasized that, with the P91 electrode used in the present work, tempering at 730 °C even for 6 h does not provide adequate toughness satisfying the specifications. Even at 760 °C a 2 h treatment is not sufficient and tempering for 6 h is required. For reasons of economy, however, it is desirable that the required mechanical properties be obtained after a tempering treatment period not

exceeding 2 h, with most fabricators specifying a heat treatment at 760 °C for 2 h.<sup>[13]</sup>

The relatively poor ductility and toughness of the weld metal produced with the P91 electrodes employed in this study requires examination in some detail. Although the modified 9Cr-1Mo steels are intended primarily for high-temperature service, it is essential that toughness be adequate to meet pressure test requirements and ambient temperature structural loading situations. There is some evidence that filler materials matching the parent material in composition in accordance with early design specifications could result in poor weld metal toughness.<sup>[25]</sup> Some minor changes in chemical composition from that of the base material have therefore been suggested: a slight reduction in Nb content, addition of Ni up to 1%, control of Si content, *etc.*

The microstructure shown in Fig. 2(b) reveals the presence of local areas of ferrite in a martensitic matrix. The formation of small amounts of ferrite in such welds is attributed to the rapid rate of cooling of the weld, which would suppress the transformation of ferrite (formed on solidification) to austenite and later to martensite. This is especially likely if the chemical composition is enriched in ferrite stabilizers. Two empirical expressions have sometimes been suggested for estimating the tendency to ferrite retention: one is the chromium equivalent  $Cr_{eq} = \%Cr + 6\% Si + 4\% Mo + 1.5\% W + 11\% V + 5\% Nb + 12\% Al + 8\% Ti - 40\% C - 2\% Mn - 4\% Ni - 2\% Co - 30\% N - \%Cu$ , and the other is the Kaltenhauser ferrite factor FF given by  $FF = \%Cr + 6\% Si + 4\% Mo + 8\% Ti + 2\% Al + 4\% Nb - 2\% Mn - 4\% Ni - 40\% C + \%N$ .<sup>[25]</sup> It has been suggested that the occurrence of ferrite has to be reckoned with in welds with  $Cr_{eq}$  greater than 10 and FF greater than 8. For the P91 weld metal in the current study, the  $Cr_{eq}$  works out to be 6.7 and the FF works out to 4.3. Although these values are well below the empirical figures of 10 and 8, respectively, ferrite was indeed clearly observable in several local areas of the microstructure. On the other hand, there were many regions in the microstructure where ferrite was not detected. It is believed that this inhomogeneity arose because the P91 electrode used had all of the alloy content in the flux coating, and it is possible that this might have led to some compositional fluctuations along the weld. The use of alloy steel manual metal arc electrodes, in which the alloying elements are introduced through the flux coating, has been found to lead to segregation effects in earlier investigations also. For example, alloy-rich segregates observed in pipeline welds were believed to be responsible for hydrogen-assisted cold cracking.<sup>[26]</sup> The segregation itself was attributed to the alloying elements being added *via* the flux coating and particularly to the inadequate mixing of ferroalloys in the weld pool. It was suggested that the use of fine ferroalloy particles in the coating would reduce the severity of the problem and prevent the occurrence of such cracking.

The presence of ferrite in the weld is believed to be responsible for the low ductility and toughness of the P91 welds. This is because the ferrite phase contains a high percentage of Cr and Mo; while the weld metal nominally contains 9% Cr and 1% Mo, it may be expected that the ferrite could become further enriched with these elements as a result of partitioning during the transformations undergone on cooling. It is known that high-chromium ferrite—as, for example, in ferritic stainless steels—is



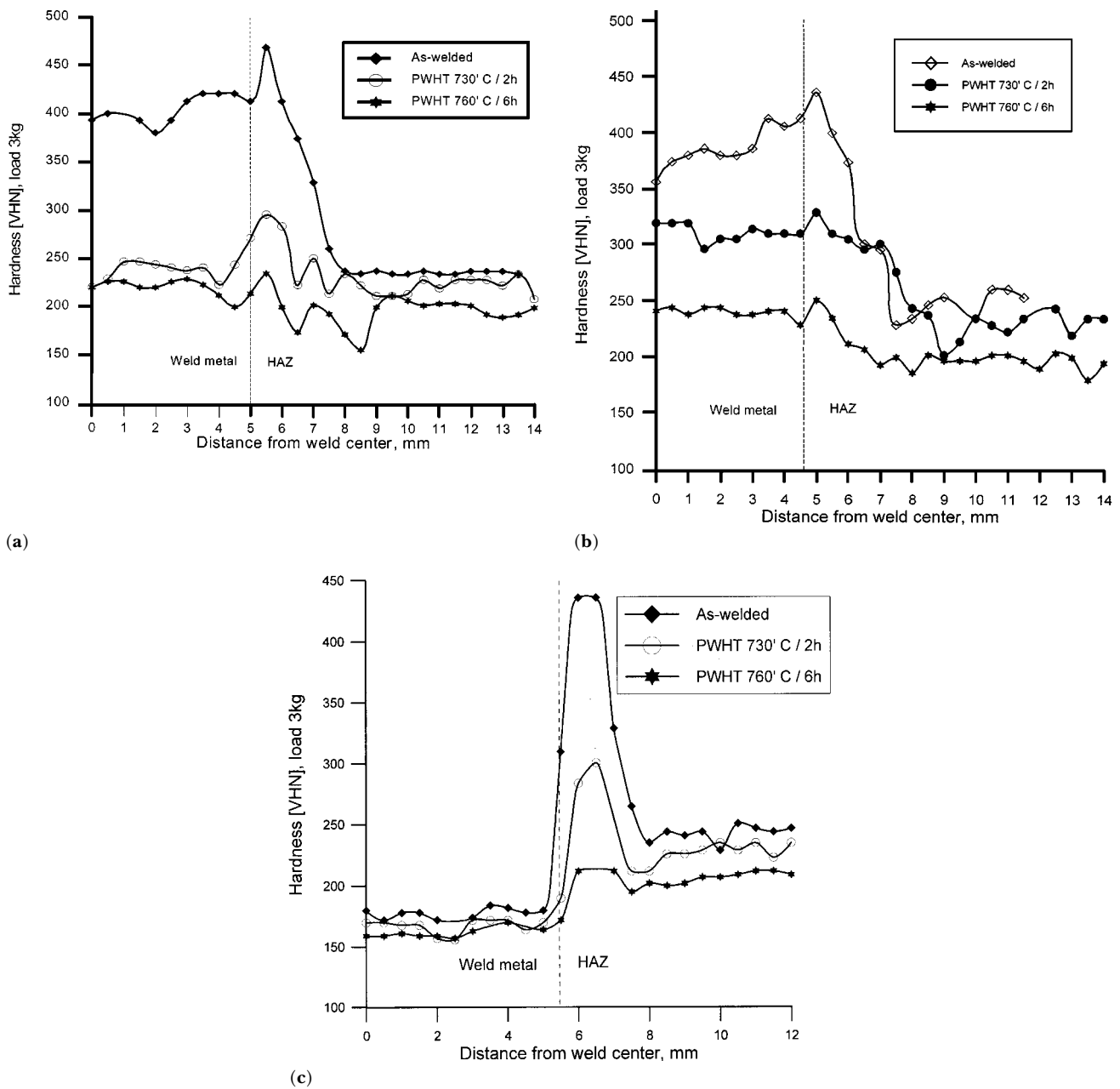


**Fig. 9** (a) Hardness profiles across the P91 weldment with P91 filler. (b) Hardness profiles across the P91 weldment with P91 filler. (c) Hardness profiles across the P91 weldment with Inconel 182 filler

**Table 2 All-weld tensile properties**

Material	Yield strength (MPa)	UTS (MPa)	Elongation (%)	Reduction in area (%)
P91 base metal	723	843	12.5	63.7
P91 weld with P91 filler	As-welded	1054	1240	6.6
	PWHT 730 °C/2 h	648	739	10.9
	PWHT 760 °C/6 h	563	647	14.1
P91 weld with P91 filler	As-welded	1199	1451	8.9
	PWHT 730 °C/2 h	873	960	8.2
	PWHT 760 °C/6 h	673	786	11.2
P91 weld with Inconel 182 filler	As-welded	283	599	39.8
	PWHT 730 °C/2 h	328	617	37.7
	PWHT 760 °C/6 h	313	640	33.7

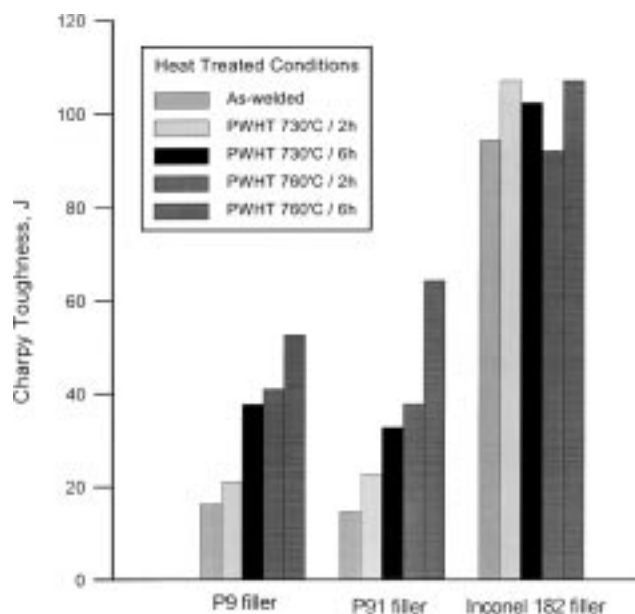


**Fig. 10** Charpy toughness of P91 weldments as a function of filler material composition and heat treatment

brittle, with an impact transition temperature that could be above room temperature unless the interstitial content is very low. The carbon content of the weld metal in the present study is 0.11% and the nitrogen content is 0.03%, (Table 1), which from this point of view are quite high. It is therefore believed that the ferrite phase, even though present only in a small amount, has been responsible for the poor weld metal toughness. It is also possible that, the presence of ferrite may lead to partitioning of carbon into the austenite, resulting in the development of a harder, more brittle martensitic structure.<sup>[25]</sup> Recent work has shown that retained  $\delta$ -ferrite could be detrimental to both weld metal toughness and creep performance.<sup>[27]</sup> The results of the present study thus confirm that, in the design of welding consumables for joining P91, the composition must be balanced such that the weld metal will be in a fully martensitic condition without any residual ferrite. Additionally, the results also show that the alloying elements should preferably be present in the core wire so that compositional fluctuations do not occur.

#### 4. Conclusions

- The as-welded martensite in the P9 and P91 weld metals gets tempered during PWHT, while the Inconel 182 fusion zone remains stable at heat treatment temperatures up to 760 °C.
- Between P9 and P91 electrodes, the latter results in much higher hardness, yield strength, and UTS. However, the toughness in the case of P9 is not superior to that of P91 when the latter is used.
- In the case of the P91 weld metal, acceptable fusion zone mechanical properties, especially ductility and toughness, are obtained only after a postweld tempering treatment at 760 °C for 6 h.

- The relatively poor ductility and toughness of the P91 welds is most likely a consequence of the presence of small amounts of ferrite in local regions of the weld metal microstructure. The ferrite islands are believed to occur because of segregation effects associated with the introduction of alloying elements through the flux coating.

#### Acknowledgments

The authors thank the Board of Research in Nuclear Sciences, Department of Atomic Energy, for the financial grant provided for this work.

#### References

1. R. Blume: *Proc. 5th Int. Conf. on Materials for Advanced Power Engineering*, Liege, Belgium, 1994, Part I, pp. 15-30.
2. T. Fujita: *Met. Progr. Mag.*, 1986, No. 8, pp. 35-40.
3. L.M. Wyatt: *Proc. Int. Conf. on Ferritic Steels for Fast Reactor Steam Generators*, S.F. Pugh and E.A. Little, eds., BNES, London, England, 1978, pp. 27-34.
4. J. Orr, F.R. Beckitt, and G.D. Fawkie: *Proc. Int. Conf. on Ferritic Steels for Fast Reactor Steam Generators*, S.F. Pugh and E.A. Little, eds., BNES, London, England, 1978, pp. 91-109.
5. V.K. Sikka, C.T. Ward, and K.C. Thomas: *Proc. Int. Conf. on Ferritic Steels for High Temperature Applications*, A.K. Khare, ed., ASM, Metals Park, OH, 1983, pp. 65-84.
6. Atsura Iseda, Minoru Kubota, Yozo Hayase, Satomi Yamamoto, and Kunihiko Yoshikawa: *Sumitomo Res.*, 1998, May (36), pp. 17-30.
7. C. Coussement and A. Dhooge: *Int. J. Pressure Vessels and Piping*, 1991, pp. 163-78.
8. J. Brozda and M. Zeman: *Welding Int.*, 1995, vol. 9 (12), pp. 33-44.
9. M.K. Booker, V.K. Sikka, and B.L.P. Booker: *Proc. Int. Conf. on Ferritic Steels for High Temperature Applications*, A.K. Khare, ed., ASM, Metals Park, OH, 1983, pp. 257-72.
10. Sadahiko Murase, Takashi Shiraishi, Yoshiki Kamemura, Tohru Mimino, and Takahiro Kanero: *Proc. Int. Conf. on Ferritic Steels for High Temperature Applications*, A.K. Khare, ed., ASM, Metals Park, OH, 1983, pp. 116-30.
11. S.K. Albert, T.P.S. Gill, A.K. Tyagi, S.L. Mannan, S.D. Kulkarni, and P. Rodriguez: *Welding J.*, 1997, vol. 76, pp. 135s-142s.
12. R. Blume, K.E. Leich, H. Heuser, and F.W. Meyer: *Stainless Steel Europe*, 1995, Apr., pp. 49-53.
13. S. Dittrich, V. Gross, and H. Heuser: *Proc. Nat. Welding Seminar*, Jamshedpur, 1994.
14. J. Brozda and M. Zeman: *Welding Int.*, 1996, vol. 10 (5), pp. 58-68.
15. Y. Tsuchida, K. Okamoto, and Y. Tokunaga: *Welding Int.*, 1996, vol. 10 (6), pp. 27-33.
16. D. Dugre, M. Julien, F. Pellicani, and J.C. Valliant: *Ferritic Steels for High Temperature Use in Boilers and Petrochemical Applications*, The P91 Book, Vallourec Industries, Cedex, France, 1992, p. 60.
17. Wendell B. Jones: *Proc. Int. Conf. on Ferritic Steels for High Temperature Applications*, A.K. Khare, ed., ASM, Metals Park, OH, 1983, pp. 116-30.
18. Wendell B. Jones, C.R. Hills, and D.H. Polonis: *Metall. Trans. A*, 1991, vol. 22A, pp. 1049-58.
19. T.W. Nelson, J.C. Lippold, and M.J. Mills: *Sci. Technol. Welding Joining*, 1998, vol. 3 (5), pp. 249-55.
20. S.J. Sanderson: *Proc. Int. Conf. on Ferritic Steels for High Temperature Applications*, A.K. Khare, ed., ASM, Metals Park, OH, 1983, pp. 65-84.
21. J.O. Nilsson, B. Lundquist, and M. Lonnberg: *Welding J.*, 1994, vol. 73, pp. 45-49.
22. M. Regev, S. Berger, and B.Z. Weiss: *Welding J.*, 1996, vol. 75, pp. 261s-268s.
23. F. Pellicani, J.C. Valliant, H. Godinot, and J. Roget: *Proc. 5th Int.*

- Conf. on Materials for Advanced Power Engineering*, D. Coutsouradis *et al.*, eds., Liege, Belgium, 1994, Part I, p. 415-24.
24. FBTR/33410/1993—Fast Breeder Test Reactor specification for the qualification of the welding consumables as proposed by IGCAR, Kalpakkam, India, 1993.
  25. A. Barnes: TWI Report No. 509/1995, TWI, Abington, UK, May 1995.
  26. J. Gouch and H. Muir: *Met. Constr.*, 1981, vol. 13 (3), pp. 150-58.
  27. Z. Zhang, A.W. Marshall, and J.C.M. Farrar: *Proc. Int. Conf. on Integrity of High-Temperature Welds*, organized by IOM Communications, I MECH E, co-sponsored by TWI, published by Professional Engineering Publishing Limited, London, and Bury, St Edmunds, United Kingdom, 1998, pp. 77-91.